

Electronic Supplementary Information (ESI)

5 Bio-inspired, multi-purpose and instant superhydrophobic-superoleophilic lotus leaf powder hybrid micro-nanocomposites for selective oil spill capture

Saravanan Nagappan,^a Jin Joo Park,^a Sung Soo Park,^a Won-Ki Lee^b and Chang-Sik Ha*^a

10 ^aPioneer Research Center for Nanogrid Materials, Department of Polymer Science and Engineering, Pusan National University, Busan 609-735, Republic of Korea. Fax: +82-51-514-4331; Tel: +82-10-4841-7066;
E-mail: csha@pusan.ac.kr

^bDepartment of Polymer Engineering, Pukyong National University, Busan 608-739, Republic of Korea.

15 Supplementary text

Fourier transform infrared spectroscopy analysis

Figure S2 presents the FTIR spectra of dried LL (front surface), LL powder, PMHS, PMHOS, LLP, PSiOr and LLPPSiOr hybrid micro-nanocomposites. The dried leaf showed a broad band at 3224 cm⁻¹ due to the presence of hydroxyl groups at the leaf surface (Figure S2a). The peak at 2925 cm⁻¹ and 2850 cm⁻¹ indicated the presence of C-H asymmetric and symmetric stretching vibrations. The C=O stretching vibration of carboxylic acid with an intermolecular hydrogen bond was noted at 1760 cm⁻¹ and 1630 cm⁻¹. The -CH₃ symmetrical, -CH₃, and -CH₂ asymmetrical bending vibrations were observed at 1433 cm⁻¹ and 1380 cm⁻¹. The bending vibration of the OH group on the leaf surface was observed at 1055 cm⁻¹. The waxy crystal (carnauba wax) present on the lotus leaves also matches the above values.¹ This confirmed the presence of a waxy materials on the leaf surface.^{2,3} The prepared LL powder (KBr) exhibited small changes in the functional groups upon mixing the front and rear parts of the leaves (Figure S2b). The C=O stretching vibration was changed to 1650 cm⁻¹ with a broad peak due to inter and intra molecular hydrogen bond of the leaf powder.

30 The pristine PMHS liquid sample (KBr disc) exhibited (Figure S2c) a strong peak at 2170 cm⁻¹, a broad peak from 1010 cm⁻¹ to 1095 cm⁻¹ and a peak at 800 cm⁻¹ due to the presence of (Si-H) and (Si-

O-Si) groups in the PMHS chain. The other peaks at 880 cm^{-1} , 1260 cm^{-1} and 2960 cm^{-1} were assigned to the (Si-CH₃) group and the (C-H) stretching vibration of (-CH₃) group in (Si-CH₃). The complete disappearance of the Si-H peak at 2170 cm^{-1} confirmed the successful hydroxylation of PMHS (Figure S2d). The CH₃ stretching vibration and H-bonded Si-OH stretching peak in PMHOS were observed at 2960 cm^{-1} and 3380 cm^{-1} , respectively. PMHOS exhibits strong and weak Si-O-Si stretching peaks at 1122 cm^{-1} , 1028 cm^{-1} , 800 cm^{-1} and 450 cm^{-1} . The peak at 1267 cm^{-1} , 880 cm^{-1} and 773 cm^{-1} revealed the presence of C-H stretching vibrations of Si-CH₃ and Si-(CH₃)₃. A weak Si-OH stretching peak appeared at 970 cm^{-1} and a Si-OH deformation peak overlapped at 798 cm^{-1} .

The LLP powder showed the presence of strong Si-O-Si peaks at 1122 cm^{-1} , 1028 cm^{-1} and a weak Si-O-Si peak at 450 cm^{-1} (Figure S2e). The C-H stretching frequencies to Si-CH₃ and Si-(CH₃)₃ of siloxane polymer appeared at 1267 cm^{-1} , 875 cm^{-1} and 773 cm^{-1} . A very broad peak at 3100 cm^{-1} to 3550 cm^{-1} indicates OH groups in the silica chain (Si-OH) and lotus leaves. A strong carbonyl stretching peak of lotus leaves was observed at 1630 cm^{-1} . The PSiOr spectrum showed a broad Si-OH peak at 3150 cm^{-1} to 3600 cm^{-1} (Figure S2f). The strong Si-O-Si peak was noted at 1028 cm^{-1} . The strong peak at 1640 cm^{-1} indicated the presence of aromatic double bonds in the PSiOr. The peak at 1133 cm^{-1} revealed the presence of an insoluble aromatic adsorption peak.⁴ Figure S2g shows the spectrum of LLPPSiOr hybrid micro-nanocomposites. The addition of a small amount of PSiOr suspension to LLP suspension also showed a similar peak, as obtained in LLP. The intensity was reduced slightly at the obtained peaks. The double bonds in PSiOr and insoluble aromatic adsorption peak appeared at 1133 cm^{-1} . These results highlight the good mixing of the leaf powder with PMHOS and PSiOr suspension.

Cross sectional roughness analysis

The cross sectional views of LL powder, PMHOS, LLP, PSiOr and LLPPSiOr hybrid micro-nanocomposites samples dispersed in their respective solvents were analyzed after casting onto the carbon tape surface, dried at room temperature and gold sputtered prior to analysis. The HR-SEM

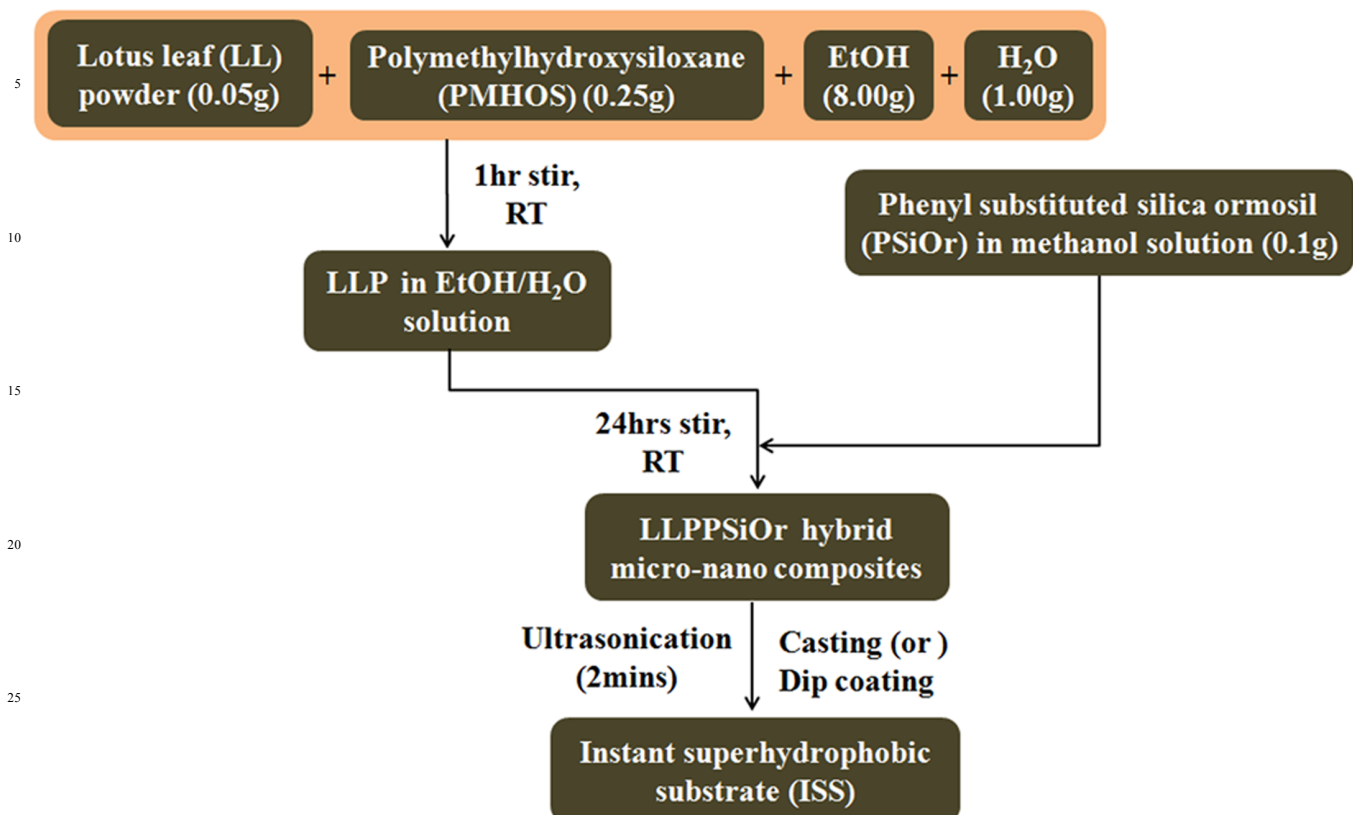
images of the samples showed the enhancement of surface roughness by the introduction of PMHOS and PSiOr to the LL powder suspension (Fig. S4). The higher surface roughness of the LLPPSiOr hybrid micro-nanocomposites may exhibit superhydrophobic properties instantaneously.

Various effects on the preparation of hybrid micro-nanocomposites

The hybrid preparation process was tested kinetically in six different cases. In the first case, the effects of LL powder dispersed in various solvents (methanol (MeOH), ethanol (EtOH), 1-propanol (1-PrOH), toluene, benzene, p-xylene, cyclohexane, octane and benzyl alcohol) were analyzed. The solution was sonicated for 2 min and casted on a glass substrate dried at room temperature and the CA of a sessile droplet was measured. The casted substrate showed hydrophobic as well as hydrophilic nature to various solvents due to the polar and non-polar nature of solvents (Figure S7a, Table S3). In the second case, the effect of PMHOS was tested with the same solvents. The casted PMHOS showed good superhydrophobicity and dispersibility for all solvents (Figure S7b, Table S3). In the third case, the leaf powder was mixed with PMHOS with the same solvents used in LL powder and PMHOS. The LLP suspension showed good dispersibility with only some polar protic solvents, such as MeOH, EtOH and 1-PrOH. In the case of the other solvents, the dispersibility was not good and more aggregate-paste was observed on the bottom of the solvents (Table S3). The CAs of the obtained LLP suspension (after sonication) showed hydrophilic to partial hydrophobic properties on the surface (Figure S7c). The superhydrophobicity was obtained for benzene in the case of PMHOS, whereas the dispersibility was not as good. These results may support the hydrophilic to partial hydrophobic properties of the LLP suspension (Figure S7c). In the fourth case, the hybrid micro-nanocomposites were prepared by mixing the LL powder, PMHOS and PSiOr suspension with some polar protic solvents, such as MeOH, EtOH and 1-PrOH. The SCA of the dispersed hybrid was measured before and after ultrasonication for 2 min followed by casting on a glass substrate (Figure S7d, Table S3). The hybrid exhibited excellent superhydrophobicity instantaneously upon the addition of a small amount of PSiOr suspension to the LLP suspension. The superhydrophobic nature was obtained both before and

after sonication. The slight improvement in the superhydrophobicity after sonication is due to the good dispersion and distribution of hybrid upon sonication. In the fifth case, the effect of silica ormocils on the preparation of hybrid micro-nanocomposites was tested. MTMS and MTES were also used to prepare silica ormocils instead of PTES. The methyl substituted silica ormocils obtained are indicated as MeSiOr 1 (MTMS), and MeSiOr 2 (MTES). The hydrophilicity of the LLP suspension was improved to hydrophobic by the addition of MeSiOr 1 ($126^\circ \pm 3^\circ$) and MeSiOr 2 ($142.83^\circ \pm 3^\circ$). The surface became superhydrophobic ($177.87^\circ \pm 1^\circ$) instantaneously by the addition of PSiOr suspension (Figure S7e), which might be due to the combination of bulky hydrophobic methyl and phenyl groups, as well as the enhanced roughness in the LLPPSiOr hybrid micro-nanocomposites. In the sixth case,
¹⁰ hybrid micro-nanocomposites of LL powder and PSiOr suspension by the addition of some polymers and monomers instead of PMHOS were tested. The prepared hybrid exhibited hydrophilicity for poly(tetrafluoroethylene) (PTFE) (60 wt% dispersion in water)/LL powder/PSiOr hybrid and for GO/LL powder/PSiOr hybrid. On the other hand, the PDMS-diol/LL powder/PSiOr hybrid exhibited hydrophobicity on the substrate. Similar hydrophobicity was also obtained for other hybrids of LL
¹⁵ powder/PSiOr with poly(methyl methacrylate) (PMMA), poly(vinylidene fluoride) (PVDF) and diphenylsilanediol (DPSD) monomer instead of PMHOS. Figure S7f shows the CA values of the obtained hybrid micro-nanocomposites.

The above six cases illustrate a clear route to prepare instant superhydrophobic hybrid micro-nanocomposites. These results showed that the superhydrophobic property depends mainly on
²⁰ PMHOS. PMHOS alone could not exhibit superhydrophobicity even when mixed with the LL powder. This means that the addition of a small amount of PSiOr suspension (0.1 g) to the LLP suspension is necessary for the enhancement of adhesive properties on the casted glass substrate in order to produce a superhydrophobic hybrid micro-nanocomposites surface. The above three combinations in the hybrid may produce instant superhydrophobic properties on any substrate.



Scheme S1. Preparation of instant superhydrophobic hybrid micro-nanocomposites (LLPPSiOr).

35

40

45

50

55

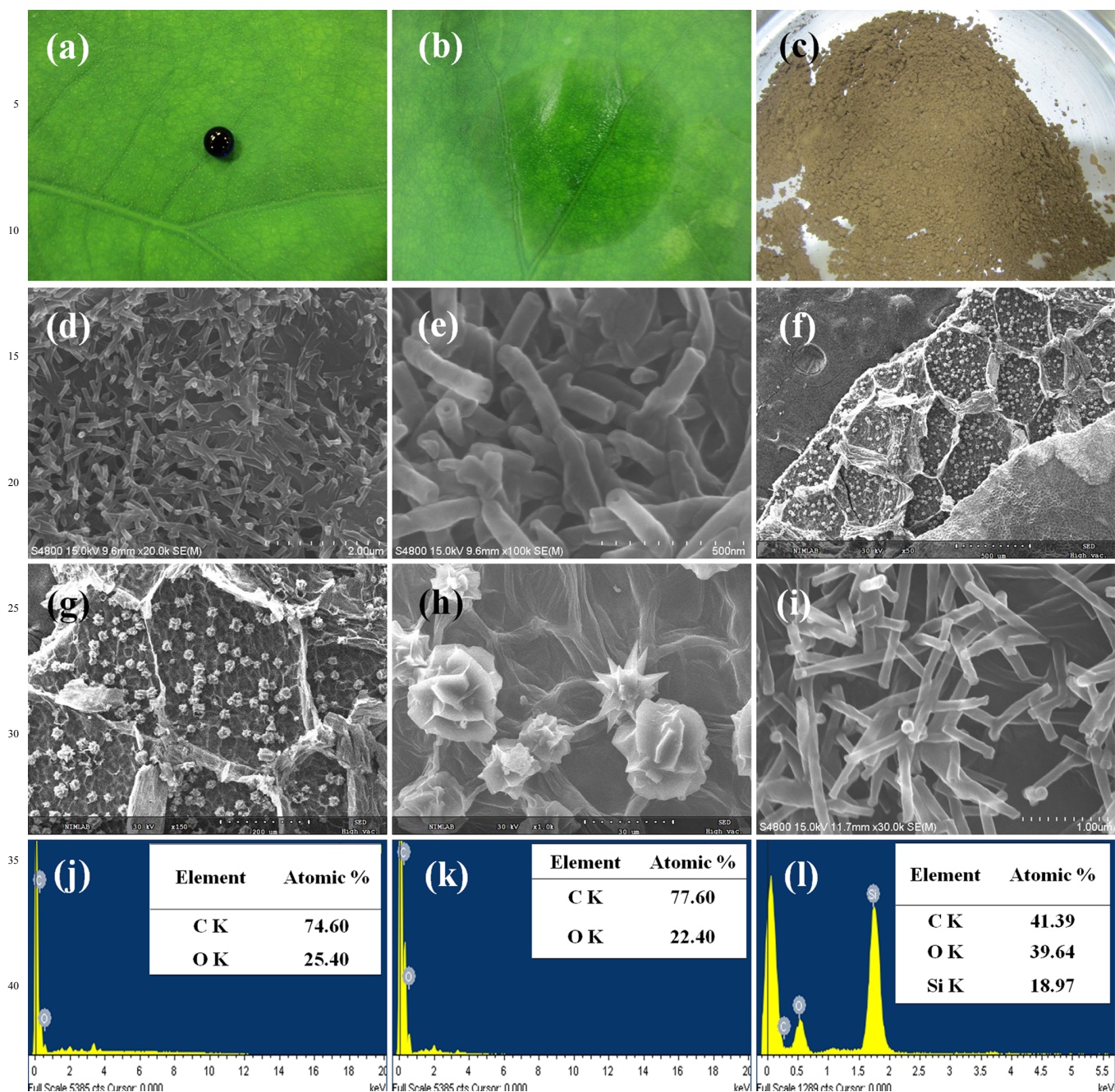


Figure S1. (a) Superhydrophobicity of LL at the front surface. (b) Superoleophilicity of LL at the front surface of the leaf to dodecane oil. (c) LL powder prepared at room temperature. (d and e) HRSEM images of a LL at the front surface clearly indicate a tubular hollow nano hair morphology (< 22 nm in hollow diameter and 70 to 82 nm in nano hair thickness). (f-h) LRSEM images of a LL at the rear surface (edge of broken leaf) indicate microhexagons with beltlike nanostructures and flower like micro papillae's in the microhexagons. (i) HRSEM image of LL at the rear surface also indicates hollow nano hair morphology (~34 nm in hollow diameter and ~107 to 137 nm in nano hair thickness). (j-l) HRSEM-EDS analysis of LL front surface, LL powder, and LLPPSiOr hybrid micro-nanocomposites.

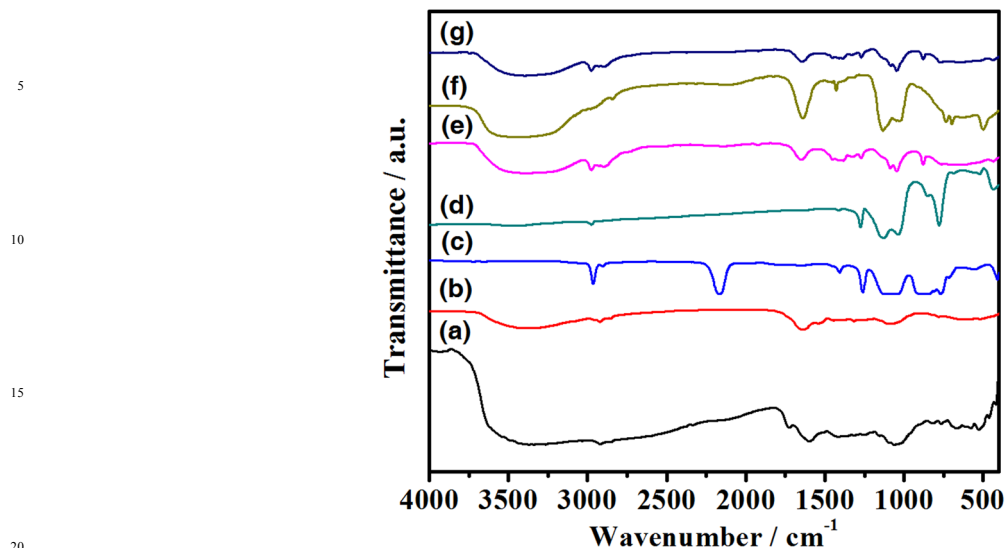


Figure S2. FTIR spectra of (a) dried LL (front surface), (b) LL powder, (c) PMHS, (d) PMHOS, (e) LLP, (f) PSiOr and (g) LLPPSiOr hybrid micro-nanocomposites.

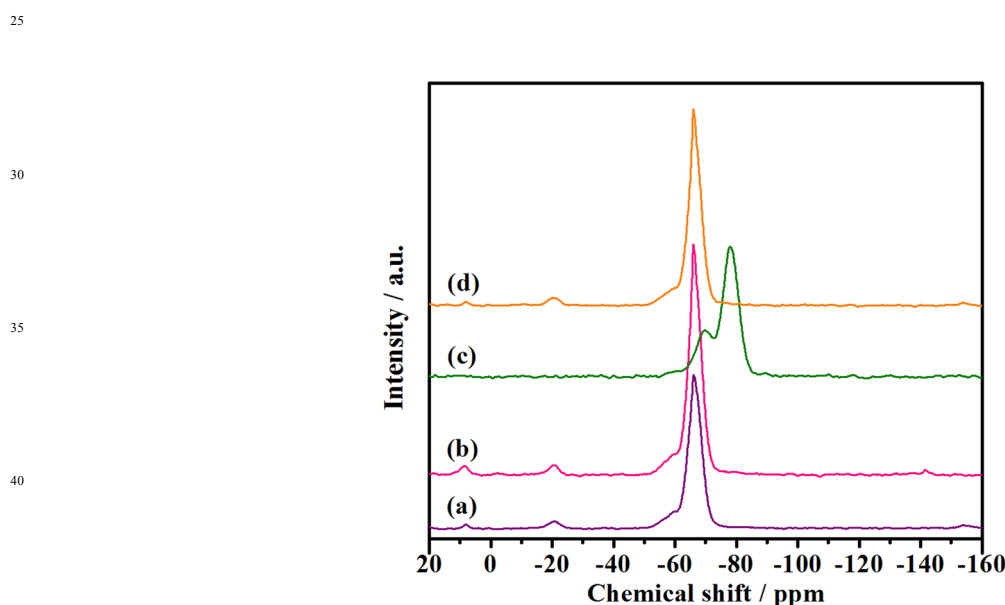


Figure S3. ²⁹Si CP MAS NMR spectra of (a) PMHOS, (b) LLP, (c) PSiOr and (d) LLPPSiOr hybrid micro-nanocomposites.

5

10

15

20

25

30

35

40

50

55

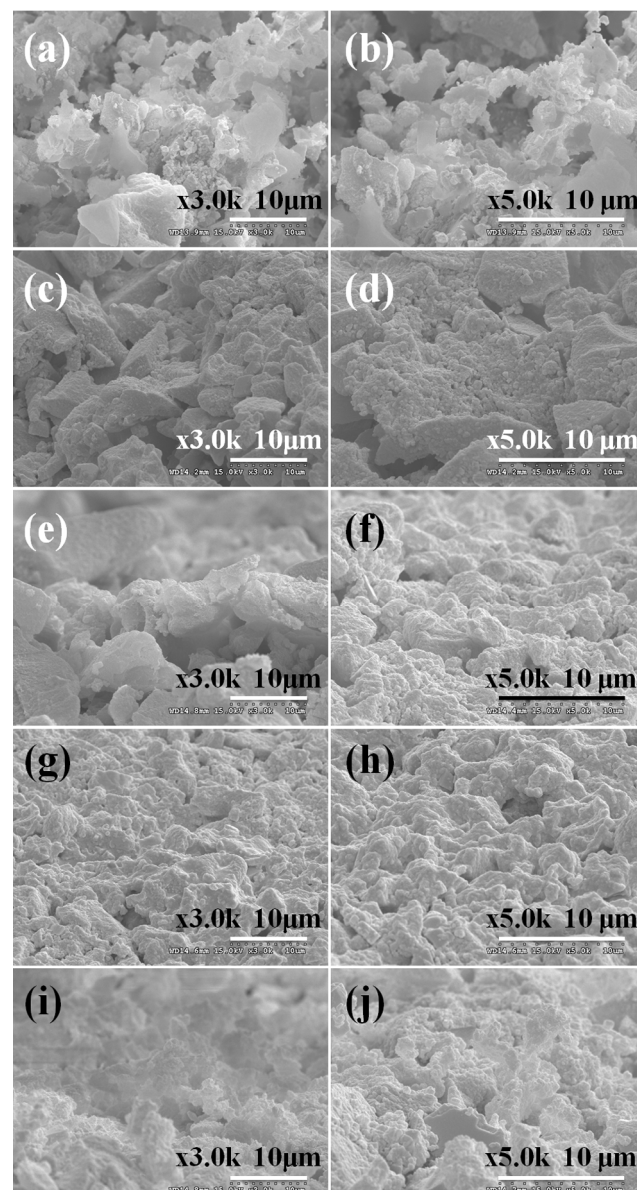
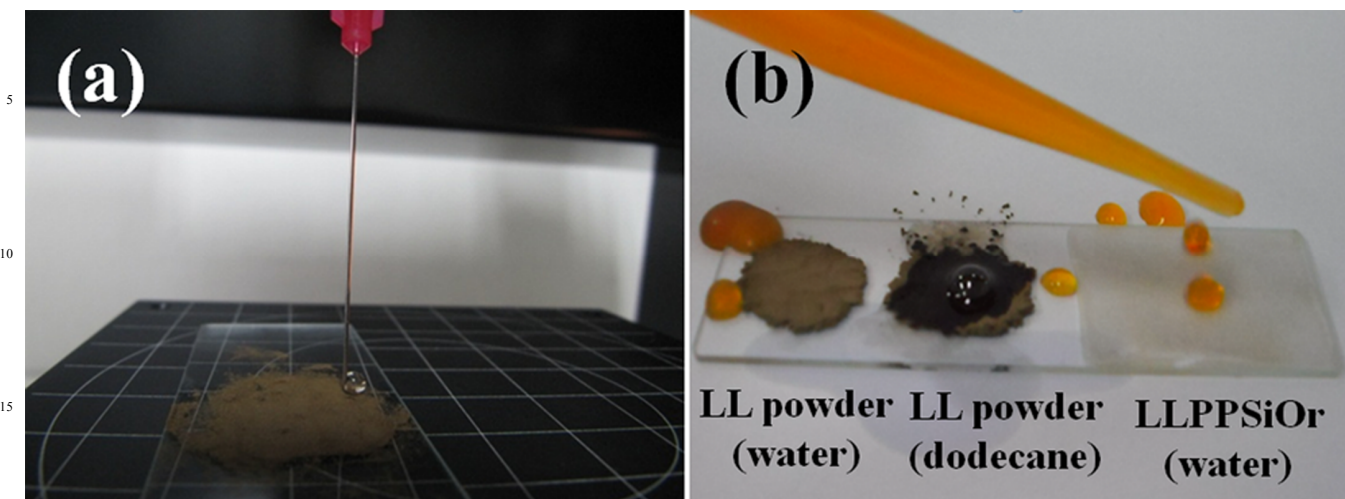
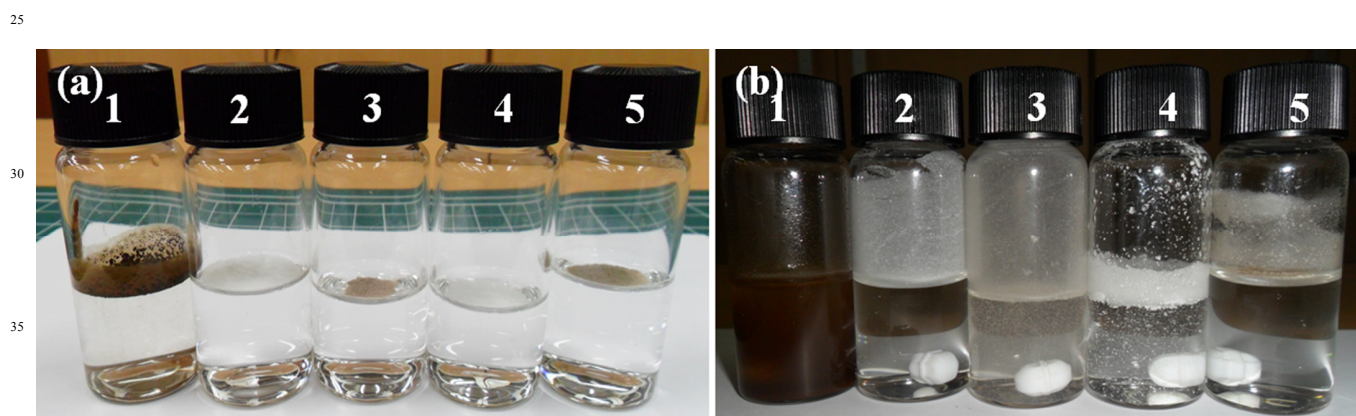


Figure S4. HRSEM surface roughness images at the side views of (a and b) LL powder, (c and d) PMHOS and (e and f) LLP, dispersed in ethanol. (g and h) PSiOr dispersed in methanol. (i and j) LLPPSiOr hybrid micro-nanocomposites dispersed in ethanol/methanol.



20 **Figure S5.** (a and b) Superhydrophobicity of LL powder to water under the aggregation of bulk powder. (b) Superoleophilicity of LL powder to dodecane and superhydrophobicity of LLPPSiOr hybrid micro-nanocomposites to water.



25 **Figure S6.** Optical images of LL powder, PMHOS, LLP, PSiOr, and LLPPSiOr hybrid powders (1-5) in water at (a) before and (b) after stirring for 24 h. The LL powder exhibited superhydrophobicity on the water surface without applying a physical force (before stirring). On the other hand, a partial hydrophobic and hydrophilic dispersion was obtained after stirring the solution from a few hours to 24 h in water ((a)1 and (b)1)). This is due to the presence of hydrophilic functional groups at LL powder. Complete superhydrophobicity of PMHOS and LLPPSiOr, and partial distribution of LLP and PSiOr were obtained after stirring for 24 h in water.

40

45

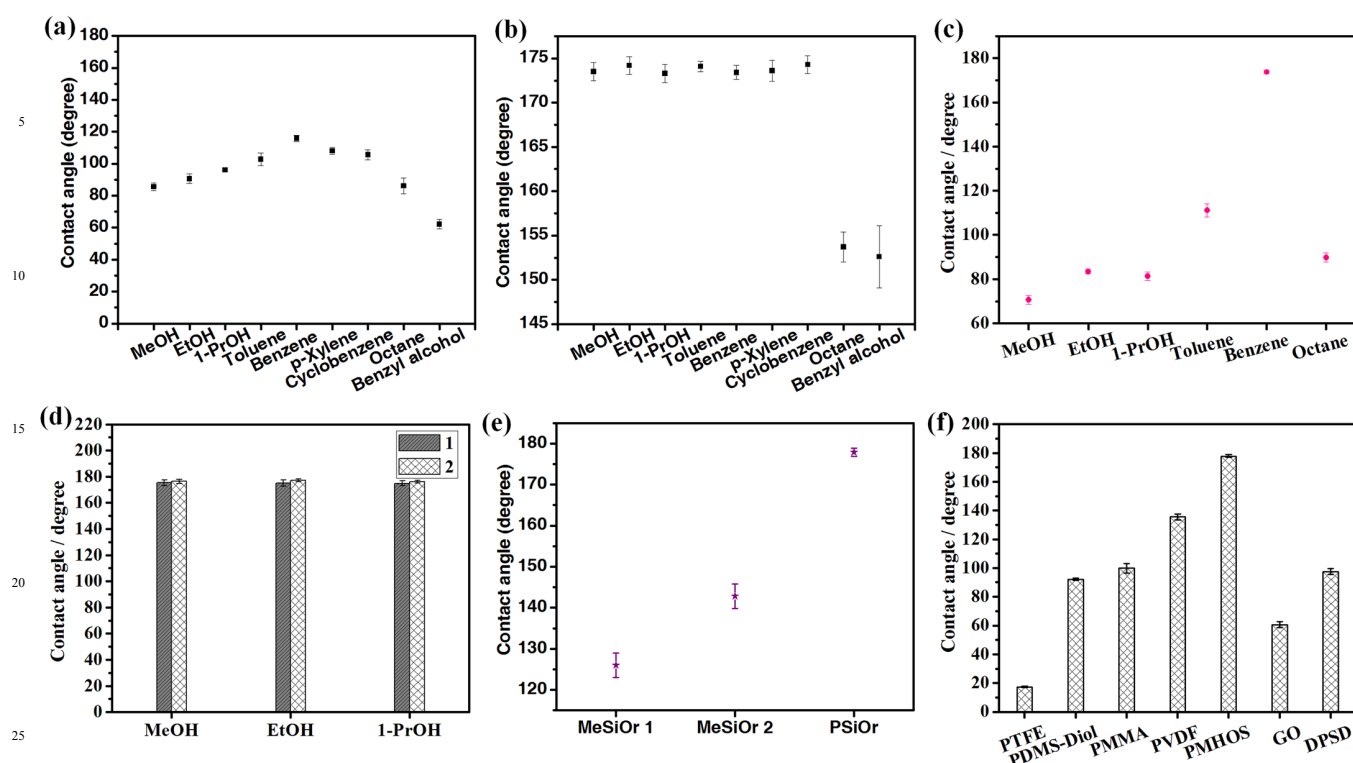


Figure S7. (a-c) Solvent effects on the SCA of various samples; LL powder, PMHOS and LLP suspension in various solvents. (d) SCA to LLPPSiOr hybrid before (1) and after (2) sonication (5 min) in MeOH, EtOH and 1-ProH. (e and f) SCA on the effect of silane precursors, various polymers and monomers instead of PMHOS on the preparation of hybrid micro-nanocomposites.

35

40

45

50

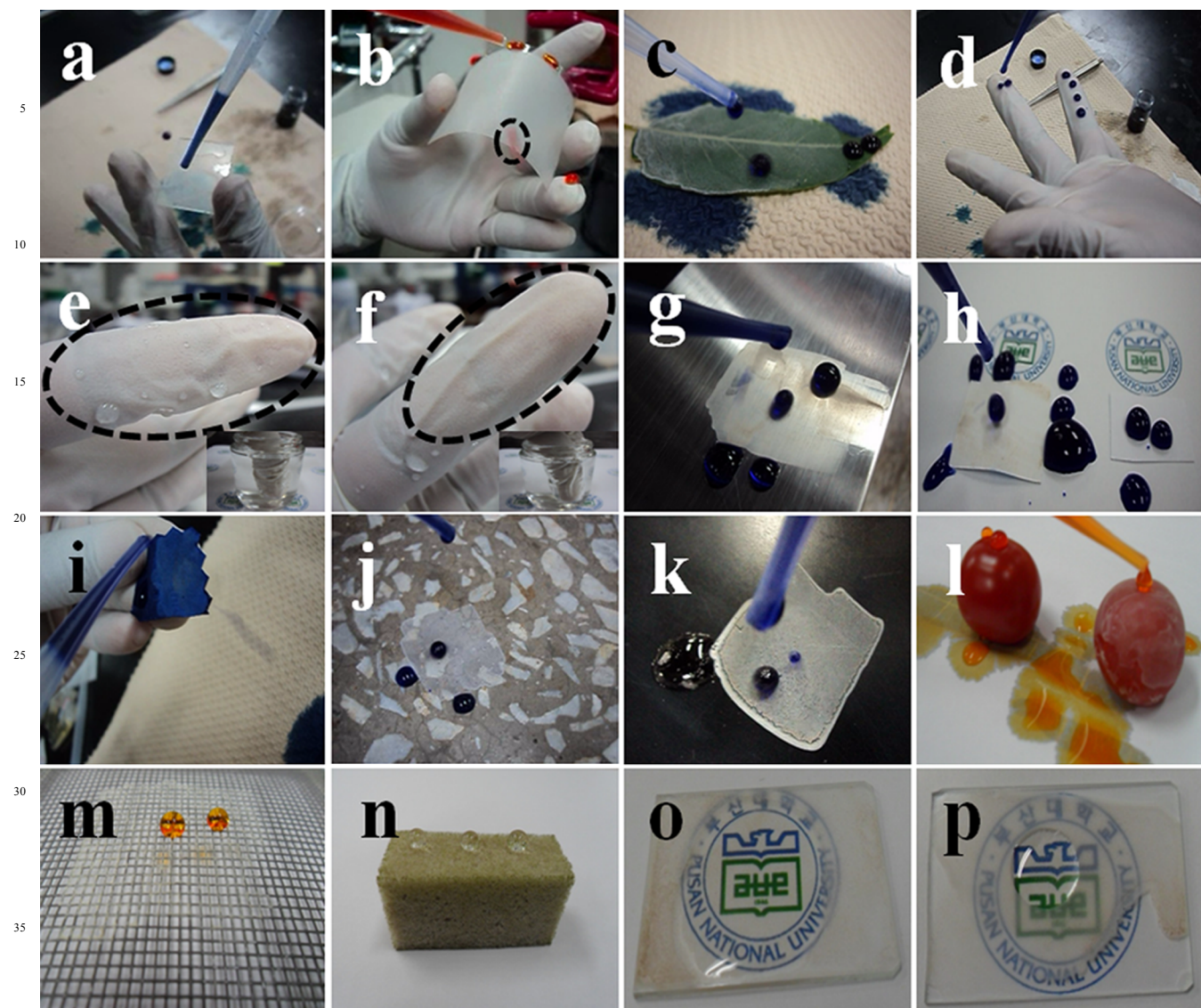


Fig. S8. Instant superhydrophobic properties of the hybrids on various substrates, such as (a) glass, (b) flexible laminating film, (c) tree leaf and (d) hand clove. (e and f) Hand clove immersed in water before and after casting (attraction and reflection of uncasted and casted finger in water). (g) Stainless steel plate, (h) paper, (i) cotton cloth, (j) cement floor, (k) wooden board, (l) cherry tomato and (m) fiber glass mesh (pore diameter, 1.5 mm). (n) Superhydrophobicity of the dip-coated hybrid/PDMS sponge dried at room temperature. (o and p) Superoleophilicity of the hybrid casted glass substrate for dodecane and soybean oil.

5

10

15

20

25

30

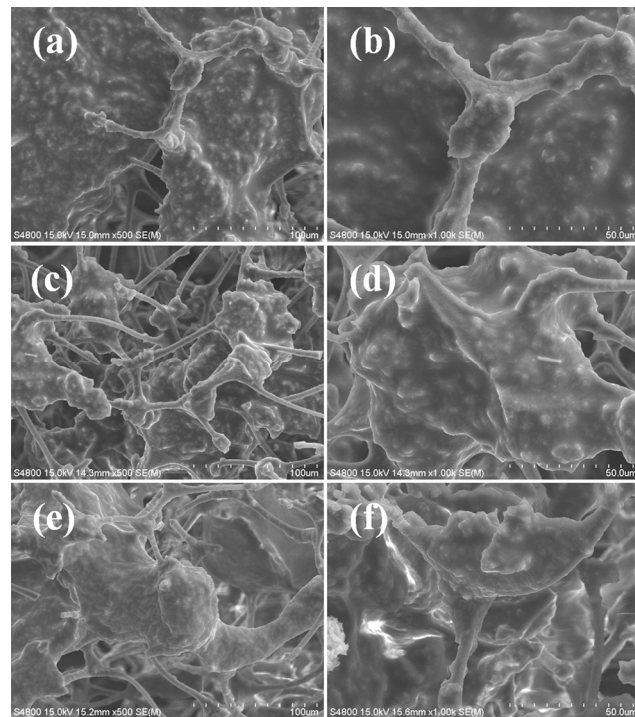


Figure S9. HRSEM surface morphology at lower and higher magnifications of the samples cured at 100°C. (a and b) Hybrid/PDMS sponge, (c and d) sponge after 1st, and (e and f) 15 cycles of oil absorptions.

35

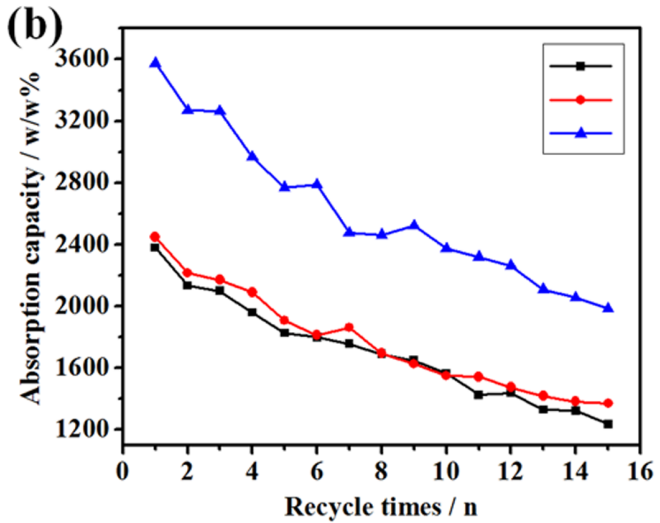
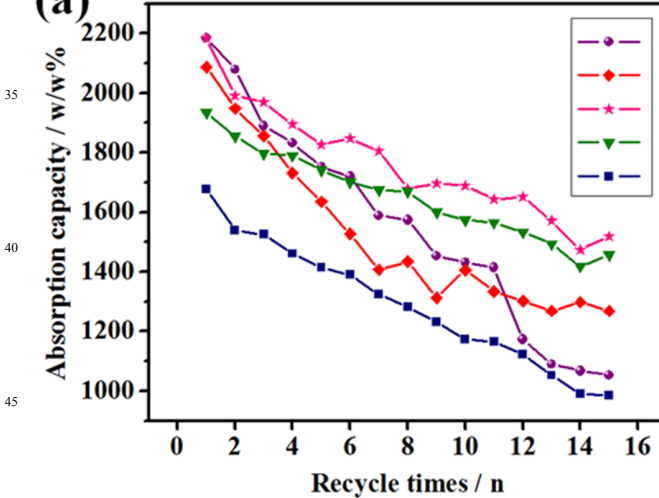


Figure S10. (a) Graphs of the absorption capacity to various oils (soybean (●), corn (◆), canola (★), diesel (▼) and decane oils (■)) absorbed by the dip coated hybrid/PDMS sponge cured at 100°C. (b) Graphs of the absorption capacity to various solvents (benzene (■), toluene (●) and chloroform (▲)) absorbed by the hybrid/PDMS sponge cured at 100°C.

50

Table S1. ^{29}Si CP MAS NMR spectral datas of PMHOS, LLP, PSiOr and LLPPSiOr hybrid micro-nanocomposites.

Sample	PMHOS	LLP	PSiOr	LLPPSiOr
Chemical shift (ppm)	8.31 (M^1) -55.89 (T^2) -59.25 (T^2') -66.11 (T^3)	8.34 -55.37 - -66.04	- -59.67 (T^1) -69.78 (T^2) -78.03(T^3)	7.98 - - -66.03

Note: (M^1) - $\text{R}_3(\text{SiO})$, (T^1) - $\text{RSi}(\text{SiO})(\text{OH})_2$, (T^2 , T^2') - $\text{RSi}(\text{SiO})_2(\text{OH})$, (T^3) - $\text{RSi}(\text{SiO})_3$, (R) - $\text{CH}_3\text{C}_6\text{H}_5$.⁴⁷

Table S2. BET surface areas, pore volumes, and pore diameters of the LL powder, PMHOS, LLP and LLPPSiOr hybrid micro-nanocomposites.

Sample	BET surface area (m^2g^{-1}) (a)	Total pore volume (cm^3g^{-1})	BJH pore diameter (nm) (b)
LL powder	2.27	0.01	-
PMHOS	413.11	1	25.2
LLP	330.32	1.05	26.3
LLPPSiOr	342.58	1.02	29.5

Note: (a) - BET: Brunauer-Emmett-Teller, (b) - BJH: Barrett-Joyner-Halenda.

Table S3. Dispersibility of PMHOS, LLP and LLPPSiOr hybrid micro-nanocomposites in various solvents.

Solvents	LL powder	PMHOS	LPP	LLPPSiOr
Methanol	+	+	+	+
Ethanol	+	+	+	+
1-Propanol	+	+	+	+
Toluene	+	+	-	-
Benzene	+	+	-	-
p-Xylene	+	+	-	-
Cyclohexane	+	+	-	-
Octane	+	+	-	-
Benzyl alcohol	+	+	-	-

Note: (+) Good dispersion, (-) Less dispersion or aggregate-paste formed on the bottom of the solvent.

Movie S1.

Superhydrophobic and superoleophilic properties of bulk LL powder spread into the glass substrate.
Superhydrophobic properties of LLPPSiOr hybrid micro-nanocomposites on glass substrate.



Movie S1.wmv

Movie S2.

Non-adhesion and free rotation (external air created by ventilation fan at the measuring room) of a water drop at the casted substrate cured at room temperature.



Movie S2.wmv

Movie S3.

Instant superhydrophobic coating at various substrates by evaporation of the solvents at room temperature (glass, laminating film, tree leaf, hand clove immersed into water at before and after casting, stainless steel plate, paper, and cotton cloth).

15



Movie S3.wmv

Movie S4.

Free movements of the substrate (from left to right and right to left) with a water droplet on the thermally cured substrates (100°C and 400°C for 5 h). Superhydrophobic (500°C for 5 h, left) to superhydrophilic changes at the substrate cured at 600°C for 5 h (right).

25



Movie S4.wmv

Movie S5.

Absorption of water and water/diesel oil by the pristine melamine sponge. Absorption of a diesel oil spill in deionized water by the dip coated hybrid/PDMS sponge substrate.

30



Movie S5.wmv

References

- 1 Y. T. Cheng, D. E. Rodak, C. A. Wong and C. A. Hayden, *Nanotechnology*, 2006, **17**, 1359.
- 2 K. Koch, A. Domisse and W. Barthlott, *Cryst. Growth Des.*, 2006, **6**, 2571.
- 3 B. Bhushan, Y. C. Jung and K. Koch, *Langmuir*, 2009, **25**, 3240.
- 4 C. Pakjamsai, N. Kobayashi, M. Koyano, S. Sasaki and Y. Kawakami, *J. Polym. Sci., Part A: Polym. Chem.*, 2004, **42**, 4587.
- 5 A. Shimojima and K. Kuroda, *Angew. Chem., Int. Ed.*, 2003, **42**, 4057.
- 6 D. Yang, Y. Xu, W. Xu, D. Wu, Y. Sunb and H. Zhu, *J. Mater. Chem.*, 2008, **18**, 5557.
- 7 T. Jermouni, M. Smahi and N. Hovnanian, *J. Mater. Chem.*, 1995, **5**, 1203.